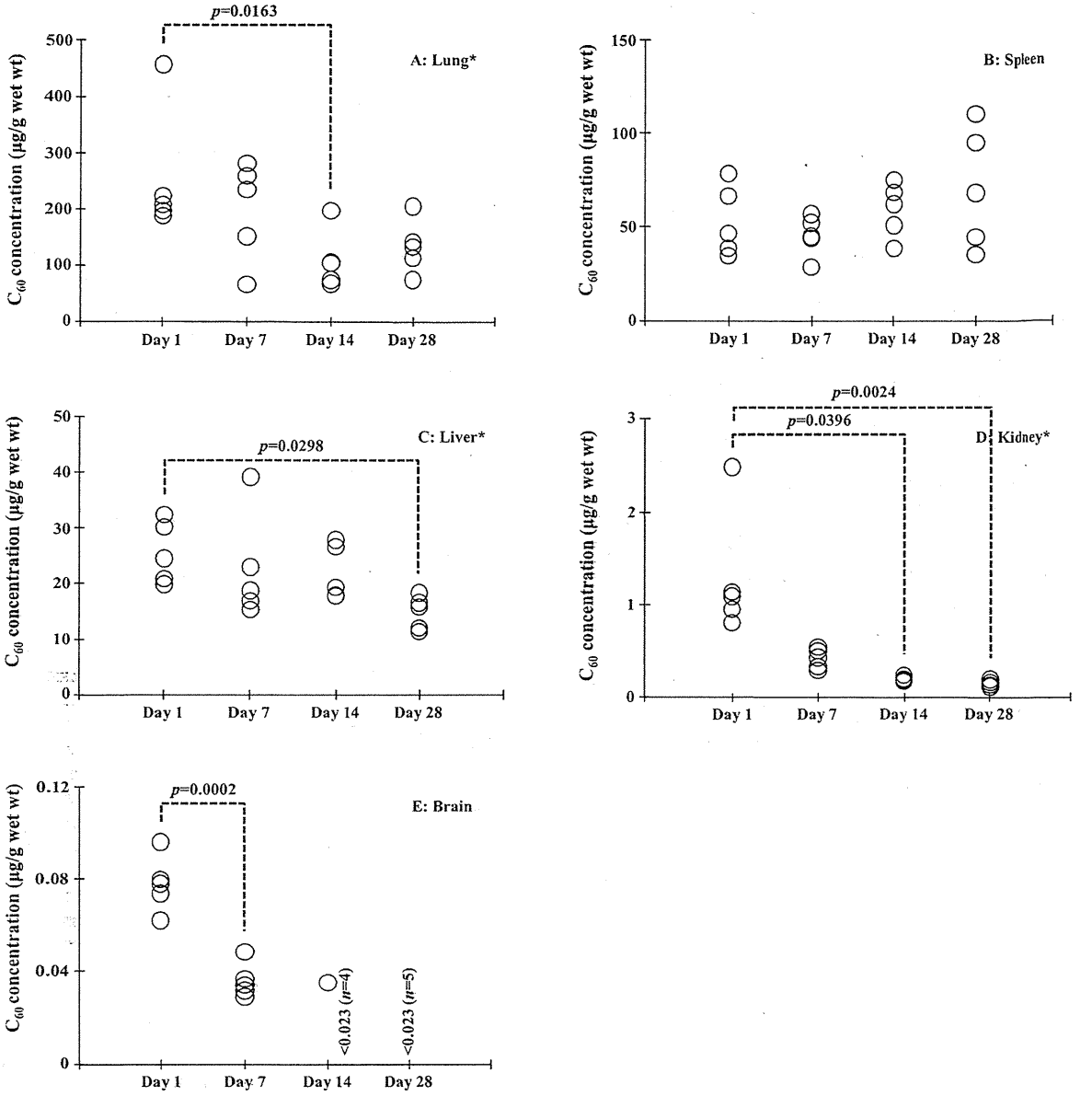

Fig. 4. Comparison of C_{60} concentrations in each tissue of the four treated rat groups (Days 1, 7, 14, and 28). Kruskal–Wallis test was used for validation of difference in the C_{60} concentrations in four tissues among treated groups and significant difference (*) was observed in lungs ($p = 0.0493$), liver ($p = 0.0251$), and kidneys ($p = 0.0007$). (A) C_{60} concentration in lungs (Day 14 vs. Day 1, $p = 0.0163$ (Mann–Whitney's *U*-test)). (B) C_{60} concentration in spleen. (C) C_{60} concentration in liver (Day 28 vs. Day 1, $p = 0.0298$ (Scheffe's test)). (D) C_{60} concentration in kidneys (Day 14 vs. Day 1, $p = 0.0396$ (Scheffe's test); Day 28 vs. Day 1, $p = 0.0024$ (Scheffe's test)). (E) C_{60} concentration in brain (Day 7 vs. Day 1, $p = 0.0002$ (Student's *t*-test)).

in lungs and liver decreased gradually. This difference of decreasing trends among tissues could be due to differences in accumulation levels. The low concentration of C_{60} in the kidneys and brain might be easily decreased compared to the high concentrations of C_{60} in the lungs, liver, and spleen. Although it is not clear whether C_{60} is excreted from the body, we propose some possible mechanisms for the decrease of C_{60} in tissues. The first possible mechanism is redistribution to other tissues via blood. Although only five tissues were examined in this study, C_{60} might be detectable in other organs. Cagle et al. (1999) reported a comparatively high concentration of water-soluble radioactive metallofullerene in bone. Moreover, although the accumulation levels were low, radiolabeled nano C_{60} (^{125}I-nanoC_{60}) was found in intestines and bone of rats (Nikolić et al., 2009). Although the C_{60} concentration in blood was below the limit of detection, the small blood volume used for the analysis could be the reason for this result. If a larger volume of blood were analyzed, C_{60} might be detected. Bullard-Dillard et al. (1996) reported that 0.39% of ^{14}C-labeled C_{60} was detected in blood of rat at 120 h post-injection. The second possible mechanism is metabolism to water-soluble fullerene metabolites and excretion into urine. Although there is no information on the intravital metabolism of C_{60}, it is possible that C_{60} could be metabolized to C_{60} derivatives (e.g. fullerenol ($C_{60}(OH)_n$)) by metabolic enzymes (e.g. cytochrome P450). Hamano et al. (1995) identified the structures of $C_{60}O$, $C_{60}O_2$, and $C_{60}O_3$ formed in P450 chemical model systems and the results support the hypothesis that possibility of a biotransformation of C_{60} into more hydrophilic C_{60} derivative capable of being excreted into the urine. In this study, the renal C_{60} concentration rapidly decreased, which also supports the possibility that C_{60} is excreted from urine. The third possible mechanism is biliary

excretion of unmodified C_{60} and/or C_{60} metabolites. Because C_{60} is lipophilic, if C_{60} is excreted without metabolism, it might be via this route. Consequently, further studies are required to verify the metabolism and excretion of C_{60}. Yamago et al. (1995) reported that virtually all of the excretion of ^{14}C-labeled water-soluble C_{60} occurred via the feces and 5.4% of ^{14}C-labeled water-soluble C_{60} was eliminated into the feces after 160 h in intravenous injection experiment. Moreover, Cagle et al. (1999) also indicated that a water-soluble radioactive metallofullerene was excreted into the feces of rats.

In summary, the current study demonstrates that C_{60} after tail vein administration is widely distributed between various tissues, such as brain, kidneys, liver, lungs, and spleen of rats. Moreover, the large variability in C_{60} concentrations among tissues was found and the highest C_{60} concentration was observed in the lungs, followed by spleen, liver, kidneys, and brain. These results suggested that C_{60} injected in the tail vein could be filtered by lung capillary vessels and accumulate in the lungs prior to being distributed to other tissues. Furthermore, C_{60} not being detected in the blood indicates that clearance of C_{60} from the blood by filtration might effectively occur in the lungs. A time-dependent decrease in C_{60} concentrations was observed in all tissues, except spleen. Moreover, a decreasing trend of C_{60} levels differed among tissues, which could be due to differences in accumulation. These results suggest that unmodified C_{60} and/or C_{60} metabolites by metabolic enzymes could be excreted into feces and/or urine. In further studies, the metabolic and excretion pathways of C_{60} should be evaluated to understand the toxicokinetics of C_{60}.

Conflict of interest

The authors declare that there are no conflicts of interest.

Acknowledgement

We are grateful to Miss Rika Maekawa and Mr. Masaki Tsuji for technical support. This study was supported by H21-kagaku-ippan-008 from the Ministry of Health, Labour and Welfare, Japan.

References

Bosi, S., Da Ros, T., Spalluto, G., Prato, M., 2003. Fullerene derivatives: an attractive tool for biological applications. Eur. J. Med. Chem. 38 (11–12), 913–923.

Bullard-Dillard, R., Creek, K.E., Scrivens, W.A., Tour, J.M., 1996. Tissue sites of uptake of ^{14}C labeled C_{60}. Bioorg. Chem. 24 (4), 376–385.

Cagle, D.W., Kennel, S.J., Mirzadeh, S., Alford, J.M., Wilson, L.J., 1999. In vivo studies of fullerene-based materials using endohedral metallofullerene radiotracers. Proc. Natl. Acad. Sci. U.S.A. 96, 5182–5187.

Colvin, V.L., 2003. The potential environmental impact of engineered nanomaterials. Nat. Biotechnol. 21 (10), 1166–1170.

Dugan, L.L., Turetsky, D.M., Du, C., Lobner, D., Wheeler, M., Almli, C.R., Shen, C.K.F., Luh, T.Y., Choi, D.W., Lin, T.S., 1997. Carboxyfullerenes as neuroprotective agents. Proc. Natl. Acad. Sci. U.S.A. 94, 9434–9439.

Friedman, S.H., DeCamp, D.L., Sijbesma, R.P., Srdanov, G., Wudl, F., Kenyon, G.L., 1993. Inhibition of the HIV-1 protease by fullerene derivatives: model building studies and experimental verification. J. Am. Chem. Soc. 115, 6506–6509.

Hamano, T., Mashino, T., Hirobe, M., 1995. Oxidation of [60]fullerene by cytochrome P450 chemical models. J. Chem. Soc. Chem. Commun. 15, 1537–1538.

Kroto, H.W., Heath, J.R., O'Brien, S.C., Curl, R.F., Samlley, R.E., 1985. Nature 318 (14), 162–163.

Kubota, R., Tahara, M., Shimizu, K., Sugimoto, N., Hirose, A., Nishimura, T., 2009. Development of a liquid chromatography–tandem mass spectrometry method for the determination of fullerenes C_{60} and C70 in biological samples. Bull. Natl. Inst. Health Sci. 127, 65–68.

Moore, M.N., 2006. Do nanoparticles present ecotoxicological risks for the health of the aquatic environment? Environ. Int. 32, 967–976.

Moussa, F., Pressac, M., Genin, E., Roux, S., Trivin, F., Rassat, A., Célin, R., Szwarc, H., 1997. Quantitative analysis of C_{60} fullerene in blood and tissues by high-performance liquid chromatography with photodiode-array and mass spectrometric detection. J. Chromatogr. B 696, 153–159.

Nakamura, E., Isobe, H., 2003. Functionalized fullerenes in water. 2003. The first 10 years of their chemistry, biology, and nanoscience. Acc. Chem. Res. 36 (11), 807–815.

Nikolić, N., Vranjes-Ethurić, S., Janković, D., Ethokić, D., Mirković, M., Bibić, N., Trajković, V., 2009. Preparation and biodistribution of radiolabeled fullerene C_{60} nanocrystals. Nanotechnology 20, 385102.

Nel, A., Xia, T., Mädler, L., Li, N., 2006. Toxic potential of materials at the nanolevel. Science 3, 622–627.

Sayes, C.M., Gobin, A.M., Ausman, K.D., Mendez, J., West, J.L., Colvin, V.L., 2005. Nano-C_{60} cytotoxicity is due to lipid peroxidation. Biomaterials 26, 7587–7595.

Tokuyama, H., Yamago, S., Nakamura, E., 1993. Photoinduced biochemical activity of fullerene carboxylic acid. J. Am. Chem. Soc. 115, 7918–7919.

Xia, X.R., Monteiro-Riviere, N.A., Riviere, J.E., 2006. Trace analysis of fullerenes in biological samples by simplified liquid–liquid extraction and high-performance liquid chromatography. J. Chromatogr. A 1129, 216–222.

Yamago, S., Tokuyama, H., Nakamura, E., Kikuchi, K., Kananishi, S., Sueki, K., Nakahara, H., Enomoto, S., Ambe, F., 1995. In vivo biological behavior of a water-miscible fullerene: ^{14}C labeling, absorption, distribution, excretion and acute toxicity. Chem. Biol. 2, 385–389.

Genes and Environment, Vol. 33, No. 1 pp. 27–31 (2011)

Short communication

Fullerene (C_{60}) Is Negative in the *In Vivo Pig-A* Gene Mutation Assay

Katsuyoshi Horibata[1,5], Akiko Ukai[1], Naoki Koyama[1], Atsuya Takagi[2], Jun Kanno[2], Takafumi Kimoto[3], Daishiro Miura[3], Akihiko Hirose[4] and Masamitsu Honma[1]

[1]Division of Genetics and Mutagenesis, National Institute of Health Sciences, Tokyo, Japan
[2]Division of Toxicology, National Institute of Health Sciences, Tokyo, Japan
[3]TEIJIN Pharma Limited, Tokyo, Japan
[4]Division of Risk Assessment, National Institute of Health Sciences, Tokyo, Japan

(Received December 24, 2010; Revised January 20, 2011; accepted January 21, 2011)

Carbon nanoparticles, such as carbon nanotubes and fullerene (C_{60}), are potential candidates as leading substances in nanotechnological fields, but little is known about their safety. Here we examined *in vivo* genotoxicity of C_{60}, by performing the *Pig-A* gene mutation assay in the peripheral blood of male C57BL/6Cr mice. Mice were given single intraperitoneal injection of 3 mg of C_{60} particles in 0.5 mL suspension containing 0.1%-Tween80-saline. As a positive control for the *Pig-A* gene mutation assay, mice were given a single oral administration of *N*-nitroso-*N*-ethylurea. At 2 and 8 weeks after treatments, we analyzed CD24-negative and -positive red blood cells in peripheral blood and calculated *Pig-A* mutant frequencies. As a result, we detected no significant differences in the mutant frequencies between C_{60} treated and non-treated mice, indicating that C_{60} is negative for genotoxicity *in vivo* in the limited target tissues assessed in this study. For the full assessment, we need comprehensive whole body survey on the genotoxicity of C_{60}.

Key words: carbon nanoparticle, *in vivo* genotoxicity, *Pig-A* gene mutation assay, fullerene

Introduction

Manufactured nanomaterials are important substances in nanotechnology, and the potential human and environmental risks need to be investigated for risk assessment and management.

There are several reports on the toxicities induced by carbon nanoparticles, such as single-wall carbon nanotubes (SWCNTs), multi-wall carbon nanotubes (MWCNTs) and fullerene (C_{60}). Intraperitoneal application of MWCNTs induced mesothelioma in $p53^{+/-}$ mouse (1) and intrascrotal administration of MWCNTs induced mesothelioma in wild-type rats (2). Reports on the *in vivo* genotoxicity of C_{60}, however, are conflicting. It was reported that intratracheal instillation of C_{60} increased both mutation frequency detected by *gpt*-assay and DNA damage detected by comet assay in lung (3). Nevertheless another group showed that treatment with C_{60} by gavage has no genotoxical effect in ICR mice, using *in vivo* micronucleus test in bone marrow cells (4). These discrepancies could have been caused by differences in administration route, test method, or target organ.

Here we examined the *in vivo* genotoxicity of C_{60} using a different test system—the recently established *Pig-A* gene mutation assay (5,6). The *Pig-A* assay, a powerful tool for the evaluation of *in vivo* genotoxicity, is based on flow cytometric enumeration of glycosylphosphatidylinositol (GPI) anchor-deficient erythrocytes and has been shown to be applicable across species from rodent to monkey (5–8). With this method, we need no transgenic animals to test *in vivo* genotoxicity, but need only 1–2 μL peripheral blood (5,6). Additionally, long-term, accumulated *in vivo* genotoxic effects could be evaluated (9).

Materials and Methods

Test chemicals: Fullerene (C_{60}, Nanom purple SUH; purity >99.9%, Frontier Carbon Corporation, Tokyo, Japan) was obtained and prepared as previously described with some modifications (1). Briefly, C_{60} was suspended to physiological saline (Ohtsuka Pharmaceutical Co., Tokyo, Japan) and autoclaved. After addition of Tween 80 (Polysorbate 80 (HX), NOF Corporation, Tokyo, Japan) at a final concentration of 0.1%, solutions were subjected to sonication by ultrasonic homogenizer (VP30s, TAITEC Co. Japan). C_{60} was prepared at a final concentration of 6 mg/mL. *N*-nitroso-*N*-ethylurea (ENU, Sigma) was dissolved in PBS (pH

[5]Correspondence to: Katsuyoshi Horibata, Division of Genetics and Mutagenesis, National Institute of Health Sciences, 1-18-1 Kamiyoga, Setagaya-ku, Tokyo 158-8501, Japan. Tel: +81-3-3700-1141, Fax: +81-3-3700-2348, E-mail: horibata@nihs.go.jp

6.0) at 10 mg/mL as previously described (5).

Animal treatment: Mice were treated as described previously (1). In brief, 6 male wild-type C57BL/6Cr mice (SLC, Shizuoka, Japan) at the age of 9–11 weeks were given single i.p. injection of 3 mg/head suspension (0.5 mL) of C_{60}. Vehicle solution (0.5 mL) was given to 6 mice as negative controls. As a positive control of this study, 5 mice were given single oral administration of ENU (40 mg/kg). Peripheral bloods were withdrawn from tail vein of mice and analyzed by the *Pig-A* gene mutation assay. All mice were housed individually under specific pathogen-free conditions, with a 12 h light-dark cycle at the animal facility of NIHS. All mice were given tap water and gamma-ray irradiated CRF-1 pellets (Oriental Yeast Co., ltd.) *ad libitum*. Animal experiments were humanely conducted under the regulation and permission of the Animal Care and Use Committee of the National Institute of Health Sciences, Tokyo, Japan.

Antibodies: Anti-mouse TER119 antibody for erythroid cells staining (clone TER-119, PE-Cy7-conjugated) and anti-mouse CD24 antibody (clone M1/69, FITC-conjugated) were obtained from BioLegend.

***Pig-A* gene mutation assay in mice:** Mice *Pig-A* gene mutation assay was performed as previously described (5,8), with some modifications. In brief, EDTA/2K was dissolved in distilled water to make a 12% solution, and used as an anticoagulant. Eighteen μL of peripheral blood were mixed with 2 μL of EDTA solution. Two μL of blood/EDTA mixture was suspended in 0.2 mL of PBS, and the cells were labeled with 1 μg of each anti-mouse TER119 and anti-mouse CD24 antibodies. After incubation for 1 h in the dark at room temperature, the cells were washed once by centrifugation ($500 \times g$, 5 min), resuspended in 2 mL of PBS, and examined using a FACS Canto II flow cytometer (BD Biosciences). After gating for single cells, about 1,000,000 TER119-positive cells were analyzed for the presence of CD24 on their surface. The data were statistically compared with the corresponding solvent control using the Student's t-test.

Results

***Pig-A* gene mutation assay with mice peripheral blood:** Recent works provided that the erythrocyte-based *Pig-A* gene mutation assay is applicable across species (5–8). According to these reports, we modified the original *Pig-A* gene mutation assay and performed it with mice peripheral blood. To classify white blood cells (WBCs) and red blood cells (RBCs) in mice peripheral blood, RBCs were stained with anti-TER119 antibody. Anti-CD24 antibody was used to detect GPI-anchored protein as previously reported (8,10). The gating strategy that was used to score GPI anchor deficient RBCs population was shown in Fig. 1. Single cells including RBCs and WBCs were gated by light scatter (Fig. 1A). To exclude WBCs from this population, TER119-positive cells (Fig. 1B) were analyzed further for the presence on the cell surface of either the GPI-anchored CD24 (Fig. 1C and 1D). The gate used for CD24-negative cells was established by blood cell samples prepared without the fluorescent reagents.

***In vivo* genotoxicity tests on fullerene (C_{60}) analyzed by the *Pig-A* gene mutation assay:** At 2 and 8 weeks after the injection of C_{60} (3 mg/head) and ENU, we analyzed CD24-negative and -positive RBCs in peripheral blood. At both 2 and 8 weeks after the injection, higher amounts of CD24 deficient RBCs were observed in the ENU treated mice (Fig. 1D) as compared with the solvent control (not shown) and C_{60} treated mice (Fig. 1C), respectively. Frequencies of CD24-negative RBCs were summarized in Fig. 2. Frequency of CD24-negative RBCs was significantly increased in ENU treated mice (2 weeks after treatment; $30.12 \pm 3.54 \times 10^{-6}$, and 8 weeks after treatment; $36.64 \pm 15.71 \times 10^{-6}$). However, we detected no obvious differences in frequency of CD24-negative RBCs between C_{60} treated and non-treated mice ($0.25 \pm 0.30 \times 10^{-6}$ versus $0.42 \pm 0.19 \times 10^{-6}$ after 2 weeks and $0.82 \pm 0.54 \times 10^{-6}$ versus $1.87 \pm 1.51 \times 10^{-6}$ after 8 weeks).

These results indicated that although the *Pig-A* gene mutation assay with mouse peripheral blood was appropriately performed, C_{60} was negative for genotoxicity *in vivo* in the RBCs assessed in our study.

Discussion

We demonstrated here that C_{60} (3 mg/head) given intraperitoneally to male C57BL/6Cr mice was negative in the *Pig-A* gene mutation assay using peripheral blood, suggesting that C_{60} was not mutagenic to erythroid precursor cells or hematopoietic stem cells.

The *Pig-A* gene mutation assay is based on detections of GPI-anchored protein on the cell surface of RBCs. The *Pig-A* gene is involved in the synthesis of GPI anchors that link various protein markers to the cell surface. It is known that paroxysmal nocturnal hemoglobinuria (PNH) is caused by somatic *PIG-A* mutations in hematopoietic stem cells (HSCs) and Aerolysin-resistant HSCs from a patient with PNH exhibited clonal *PIG-A* mutations (11,12). Additionally, it is considered that the absence of GPI-anchored protein of RBCs is caused by mutations occurred in the *Pig-A* gene of nucleated erythroid precursors and/or of HSCs (6). These observations suggested that expression of GPI-anchored CD24 of RBCs is depending on the *Pig-A* gene mutations happened in erythroid precursors and/or of HSCs in bone marrows. According to this, we considered that our results, shown here using peripheral blood of mice, reflected genotoxicity of C_{60} on bone marrows.

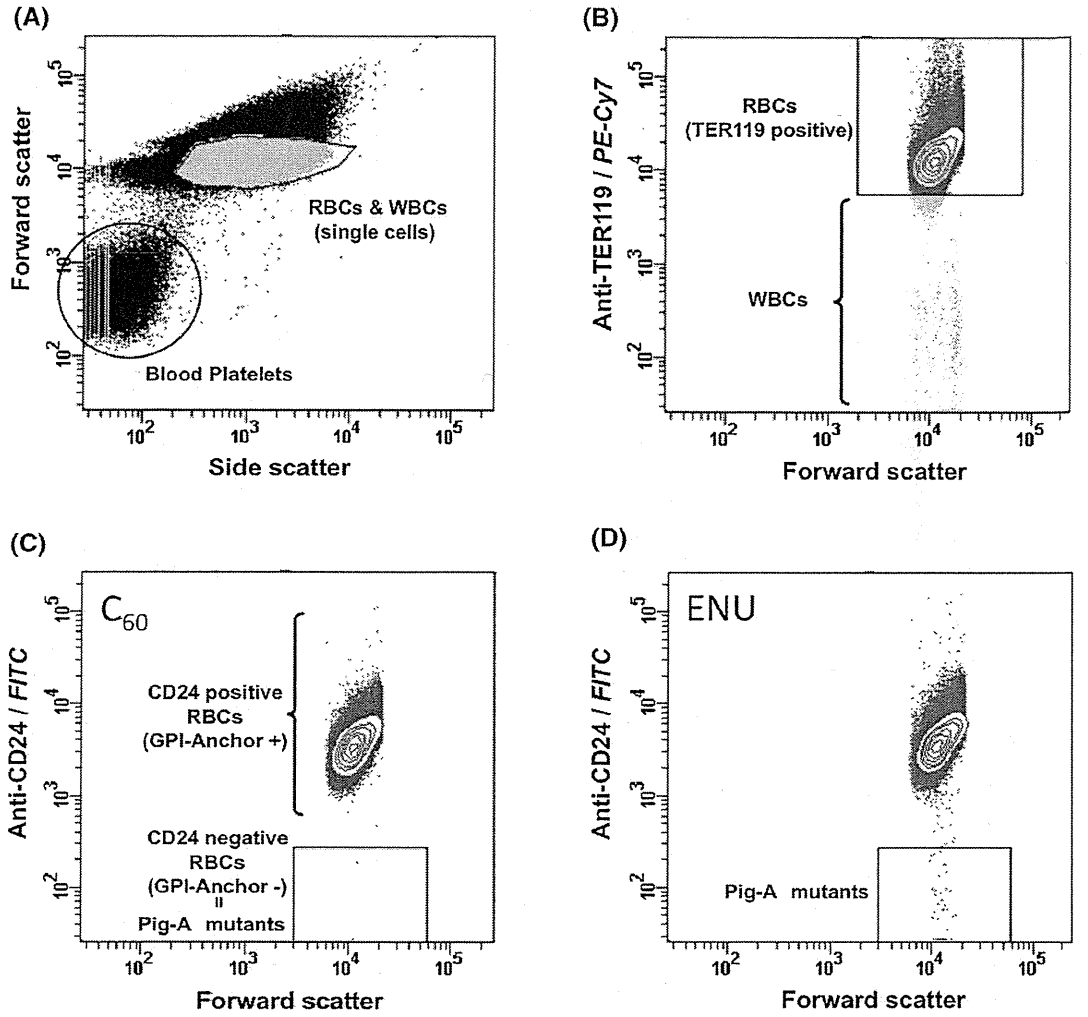

Fig. 1. Analysis of mouse peripheral blood by flow cytometry. (A) Single cell populations were gated and further analyzed with anti-TER119 antibody. (B) TER119-negative white blood cells were excluded from the gated single cell population. TER119-positive red blood cells (RBCs) were gated and further analyzed with anti-CD24 antibody. (C) Approximately 1×10^6 TER119-positive RBCs were analyzed for CD24 expression. CD24-negative RBCs (GPI-Anchor -) were scored as *Pig-A* mutants. In here, there were no obvious features in RBCs derived from C_{60} treated mice. (D) TER119-positive cells derived from ENU-treated mice were analyzed for CD24 expression.

Our data are consistent with the finding that C_{60} administered by gavage to ICR mice is negative in the *in vivo* bone marrow micronucleus test (4). These reports and our result suggest that intraperitoneal injection and gavage of C_{60} are negative for genotoxicity on bone marrow cells including erythroid precursors and HSCs. In both studies, however, the bone marrow was not exposed to C_{60} directly. A recent report showed that intratracheal instillation of C_{60} increased both mutation frequency (*gpt* assay) and DNA damage (comet assay) in the lung (3). From the mutation spectra, it was suggested that oxidative DNA damage might be involved in mutagenicity of C_{60} (3). C_{60}-phagocytized macrophages and granulomatous formations were also observed in the lung (3). Additionally, intratracheal instillation of C_{60} could induce inflammatory responses in the lung (13). It is known that reactive oxygen species (ROS) generation by nanoparticles could be due to particle-cell interactions, especially in the lungs where there is a rich pool of ROS producers like the inflammatory phagocytes, neutrophols and macrophages (14). According to these observations, it is possible that both direct exposure to the target tissue and inflammatory response are important factors in the evaluation of the genotoxicity of C_{60}.

On the other hand, details of inflammatory responses were unclear, but intraperitoneal application of C_{60} induced no obvious change on exposed area except for black patchy deposits on the serosal surfice in $p53^{+/-}$ mouse (1). Therefore it is expected that ROS generation

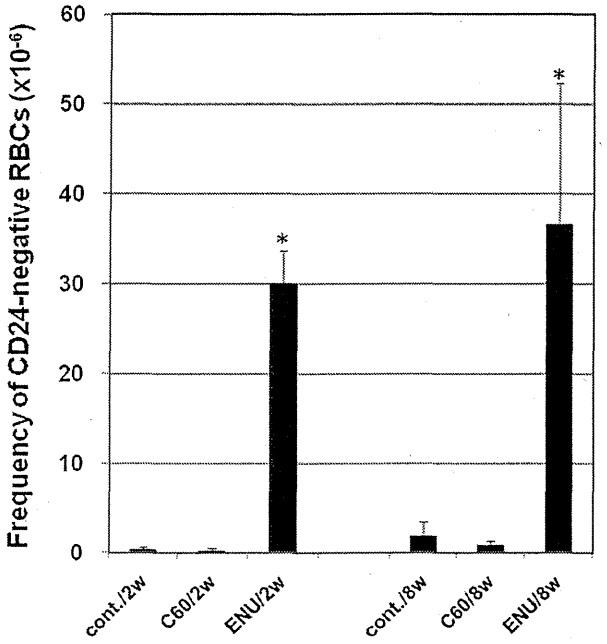

Fig. 2. Frequency of CD24-negative RBCs. At 2 and 8 weeks after mice were treated with C_{60} (3 mg/animal), ENU (40 mg/kg), or solvent, peripheral blood was withdrawn from the tail vein and RBCs were analyzed by flow cytometry for CD24 expression. Values are the mean ± SD of data from 6 animals (C_{60} and solvent) or 5 animals (ENU). *P*-values less than 0.0005 are indicated by asterisks.

by inflammatory responses might not occur and we detected negative genotoxicity in our case.

Recent reports including our results about genotoxicity of C_{60} are discrepant. However, it is known that C_{60} have an ability to quench and generate ROS (15,16). These discrepancies about genotoxicity of C_{60} may be caused by a duality of C_{60} itself. At this time, we cannot explain the mechanism(s) of C_{60} genotoxicity in detail, but we suspect that it is complex and includes oxidative DNA damages, inflammation, and other biological factors. To assess the genotoxicity of C_{60} more fully, we need a comprehensive whole body survey.

Acknowledgement: This work was supported by Health and Labor Sciences Research Grant, Japan, Grant Number: H21-chemical-general-008, and Human Science Foundation, Japan; Grant Number: KHB1006.

References

1 Takagi A, Hirose A, Nishimura T, Fukumori N, Ogata A, Ohashi N, Kitajima S, Kanno J. Induction of mesothelioma in $p53^{+/-}$ mouse by intraperitoneal application of multi-wall carbon nanotube. J Toxicol Sci. 2008; 33: 105–16.

2 Sakamoto Y, Nakae D, Fukumori N, Tayama K, Maekawa A, Imai K, Hirose A, Nishimura T, Ohashi N, Ogata A. Induction of mesothelioma by a single intrascrotal administration of multi-wall carbon nanotube in intact male Fischer 344 rats. J Toxicol Sci. 2009; 34: 65–76.

3 Totsuka Y, Higuchi T, Imai T, Nishikawa A, Nohmi T, Kato T, Masuda S, Kinae N, Hiyoshi K, Ogo S, Kawanishi M, Yagi T, Ichinose T, Fukumori N, Watanabe M, Sugimura T, Wakabayashi K. Genotoxicity of nano/microparticles in *in vitro* micronuclei, *in vivo* comet and mutation assay systems. Part Fibre Toxicol. 2009; 6: 23.

4 Shinohara N, Matsumoto K, Endoh S, Maru J, Nakanishi J. *In vitro* and *in vivo* genotoxicity tests on fullerene C_{60} nanoparticles. Toxicol Lett. 2009; 191: 289–96.

5 Miura D, Dobrovolsky VN, Kasahara Y, Katsuura Y, Heflich RH. Development of an *in vivo* gene mutation assay using the endogenous *Pig-A* gene: I. Flow cytometric detection of CD59-negative peripheral red blood cells and CD48-negative spleen T-cells from the rat. Environ Mol Mutagen. 2008; 49: 614–21.

6 Miura D, Dobrovolsky VN, Mittelstaedt RA, Kasahara Y, Katsuura Y, Heflich RH. Development of an *in vivo* gene mutation assay using the endogenous *Pig-A* gene: II. Selection of *Pig-A* mutant rat spleen T-cells with proaerolysin and sequencing *Pig-A* cDNA from the mutants. Environ Mol Mutagen. 2008; 49: 622–30.

7 Dobrovolsky VN, Shaddock JG, Mittelstaedt RA, Manjanatha MG, Miura D, Uchikawa M, Mattison DR, Morris SM. Evaluation of Macaca mulatta as a model for genotoxicity studies. Mutat Res. 2009; 673: 21–8.

8 Phonethepswath S, Bryce SM, Bemis JC, Dertinger SD. Erythrocyte-based *Pig-a* gene mutation assay: demonstration of cross-species potential. Mutat Res. 2008; 657: 122–6.

9 Miura D, Dobrovolsky VN, Kimoto T, Kasahara Y, Heflich RH. Accumulation and persistence of *Pig-A* mutant peripheral red blood cells following treatment of rats with single and split doses of *N*-ethyl-*N*-nitrosourea. Mutat Res. 2009; 677: 86–92.

10 Keller P, Tremml G, Rosti V, Bessler M. X inactivation and somatic cell selection rescue female mice carrying a Piga-null mutation. Proc Natl Acad Sci U S A. 1999; 96: 7479–83.

11 Takeda J, Miyata T, Kawagoe K, Iida Y, Endo Y, Fujita T, Takahashi M, Kitani T, Kinoshita T. Deficiency of the GPI anchor caused by a somatic mutation of the *PIG-A* gene in paroxysmal nocturnal hemoglobinuria. Cell. 1993; 73: 703–11.

12 Hu R, Mukhina GL, Piantadosi S, Barber JP, Jones RJ, Brodsky RA. *PIG-A* mutations in normal hematopoiesis. Blood. 2005; 105: 3848–54.

13 Park EJ, Kim H, Kim Y, Yi J, Choi K, Park K. Carbon fullerenes (C_{60}s) can induce inflammatory responses in the lung of mice. Toxicol Appl Pharmacol. 2010; 244: 226–33.

14 Li JJ, Muralikrishnan S, Ng CT, Yung LY, Bay BH. Nanoparticle-induced pulmonary toxicity. Exp Biol Med (Maywood). 2010; 235: 1025–33.

15 Markovic Z, Trajkovic V. Biomedical potential of the reactive oxygen species generation and quenching by

fullerenes (C_{60}). Biomaterials. 2008; 29: 3561–73.
16 Singh N, Manshian B, Jenkins GJ, Griffiths SM, Williams PM, Maffeis TG, Wright CJ, Doak SH. NanoGenotoxicology: the DNA damaging potential of engineered nanomaterials. Biomaterials. 2009; 30: 3891–914.

—Review—

ナノマテリアルの慢性影響研究の重要性

広瀬明彦,*,[a] 高木篤也,[a] 西村哲治,[a] 津田洋幸,[b] 坂本義光,[c]
小縣昭夫,[c] 中江　大,[c] 樋野興夫,[d] 菅野　純[a]

Importance of Researches on Chronic Effects by Manufactured Nanomaterials

Akihiko HIROSE,*,[a] Atsuya TAKAGI,[a] Tetsuji NISHIMURA,[a]
Hiroyuki TSUDA,[b] Yoshimitsu SAKAMOTO,[c] Akio OGATA,[c]
Dai NAKAE,[c] Okio HINO,[d] and Jun KANNO[a]

[a]Division of Risk Assessment, National Institute of Health Sciences, Kamiyoga 1-18-1, Setagaya-ku, Tokyo 158-8501, Japan, [b]Nagoya City of University, 1 Kawasumi Mizuho-cho, Mizuho-ku, Nagoya 467-8601, Japan, [c]Tokyo Metropolitan Institute of Public Health, 3-24-1 Hyakunin-cho, Shinjyuku-ku, Tokyo 169-0073, Japan, and [d]Juntendo University School of Medicine, 2-1-1 Hongo, Bunkyo-ku, Tokyo 113-8421, Japan

(Received September 3, 2010)

Manufactured nanomaterials are the most important substances for the nanotechnology. The nanomaterials possess different physico-chemical properties from bulk materials. The new properties may lead to biologically beneficial effects and/or adverse effects. However, there are no standardized evaluation methods at present. Some domestic research projects and international OECD programs are ongoing, in order to share the health impact information of nanomaterails or to standardize the evaluation methods. From 2005, our institutes have been conducting the research on the establishment of health risk assessment methodology of manufactured nanomaterials. In the course of the research project, we revealed that the nanomaterials were competent to cause chronic effects, by analyzing the intraperitoneal administration studies and carcinogenic promotion studies. These studies suggested that even aggregated nanomaterials were crumbled into nano-sized particles inside the body during the long-term, and the particles were transferred to other organs. Also investigations of the toxicokinetic properties of nanomaterials after exposure are important to predict the chronically targeted tissues. The long lasting particles/fibers in the particular tissues may cause chronic adverse effects. Therefore, focusing on the toxicological characterization of chronic effects was considered to be most appropriate approach for establishing the risk assessment methods of nanomaterials.

Key words——chronic toxicity; multi-wall carbon nanotube (MWCNT); fullerene

1. はじめに

近年，ナノテクノロジーの中心的な役割を担う物質としての産業用ナノマテリアルは，急速にその種類や生産量が増加しつつあるところであるが，新たに期待されているナノマテリアルの物理化学特性については，有効的な生理活性等に使用され得る特性を持つ反面，ヒト健康影響に対する懸念についても検証されるべきであると考えられている．つまり，ナノマテリアルを用いた技術や製品を社会的に受容するためには，安全性の検証を行うことが不可欠であると思われる．しかし，従来の一般的な化学物質とは異なる物理化学的特性は，その毒性評価においても従来とは異なる考え方を取り入れることも必要とされている．それゆえ，ナノマテリアルの特性を考慮した有害性評価手法の開発が急務となっている．また，国際的な枠組みにおいても，ナノマテリアルの安全性確認は，重要な問題として認識されており，OECD や ISO 等を中心として評価手法の国際的標準化に向けた取り組みが進行しているところでもある．本稿では，ナノマテリアルの安全性評価

[a]国立医薬品食品衛生研究所（〒158-8501 東京都世田谷区上用賀 1-18-1），[b]名古屋市立大学（〒467-8601 名古屋市瑞穂区瑞穂町字川澄 1），[c]東京都健康安全研究センター（〒169-0073 東京都新宿区百人町 3-24-1），[d]順天堂大学医学部（〒113-8421 東京都文京区本郷 2-1-1）
*e-mail: hirose@nihs.go.jp

本総説は，日本薬学会第 130 年会シンポジウム S18 で発表したものを中心に記述したものである．

の確立に向けたこれらの取り組みに貢献してきたわれわれの研究成果の一部と，それらの研究結果から帰納的に導き出された慢性影響評価研究の重要性について論ずる．

2. ナノマテリアルのリスク評価法の確立における課題

一般的に，化学物質の健康影響評価（リスクアセスメント）の基本的なフレームは，有害性評価と曝露評価，及び各々の評価内容を比較・統合化する過程のリスク判定のステップから成り立っている．この基本的なフレーム自体は，ナノマテリアルの健康影響評価に適用できるものであると考えられる．[1-5] しかし，ナノマテリアルに特徴的な新たな物理化学的性質，特にサイズが生体内高分子と近いことや，高い表面活性のために凝集し易い性質を考慮すると，よりサイズの大きい通常のバルク化合物や完全に溶解した単一分子化合物とは，生体内挙動が異なることが予想され，同じ化学組成の化合物であってもその毒性発現部位や発現様式は異なることが予想される．つまり，体内動態［吸収 absorption，分布 distribution，代謝 metabolism，排泄 excretion (ADME)］情報は，一般の化学物質より重要な意味を持つと考えられる．

そこで，生体内での挙動を把握するためには，生体試料中で検出，同定・定量できる方法を確立しなくてはならない．一般にナノマテリアルの開発段階において，その性質を把握するための物理化学的測定法も同時に開発されているはずであるが，それらの手法は生体試料中に存在するナノマテリアルにそのまま適用できないことも多い．さらに，機器分析法による生体試料中での検出や定量が可能になったとしても，生体内で実際にナノの状態で存在しているのか，あるいは再凝集などはしていないかなど，標的組織における最終的な生体内反応に影響を及ぼすと考えられる実際のナノマテリアルの存在状態を把握するためには，最終的には，組織標本の電子顕微鏡などによる確認が必要となる．

一方，体内動態に影響を与える因子として，投与法を検討する必要もある．単独では凝集し易いナノマテリアルをそのまま曝露するということは，物理的に巨大となった粒子は体への吸収性が低く，ナノマテリアル自体の体内動態や懸念される有害性を検出することが困難になると考えられるためである．そのために曝露実験時におけるナノマテリアルの分散手法の開発が必要となる．職業曝露などの比較的大量のナノマテリアル曝露の安全性を評価するという観点からは，凝集したままの曝露にも意義があるかもしれないが，製品中への混入や環境中への排出を経由した，分散された曝露も想定されることは考慮すべきであると考えられる．

Figure 1 は，凝集したナノマテリアルが，生体に取り込まれた場合に想定される体内動態を模式図化したものである．ナノマテリアルの使用用途にも依存するが，製品中のナノマテリアルはポリマー等の他の高分子化合物等と混合された状態，あるいはナノマテリアルだけが単独で製品から解離していく状態を考慮しても，この凝集性のために，大きな粒子として曝露する可能性が高いものと想定される．急性的には，このサイズの大きくなった物質は生体に取り込まれることはほとんどなく，局所的な刺激を起こすような変化を除いては，生体内で有害性が惹起される可能性は低いものと考えられる．しかし，仮に凝集したナノマテリアルが長期間に渡って，吸収部位である肺胞や消化管，損傷皮膚などの局所に滞留したり，慢性的に曝露したりするケースを想定すると，時間経過とともに小さくなった凝集体の粒子を除去するために，マクロファージなどの食細胞による取り込みや，表面活性の高いナノマテリアル分子と生体成分との結合作用による侵食作用により，生体に少しずつ取り込まれることが想定される．もしも生体内に取り込まれたナノマテリアルと生体内成分との結合性が高い場合には，容易に生体外に排出されることはなく，特定の組織等へ蓄積し易くなり，慢性影響の可能性を検討する必要が出てくると想定できる．

3. 国立医薬品食品衛生研究所における取り組みの成果の概要

以上のナノマテリアル固有の検討課題を考慮して，われわれは 2005 年より厚生労働科学研究の化学物質リスク研究事業の枠組みの中で，ナノマテリアルの健康影響評価手法の開発に係わる研究を推し進めてきたところである．われわれは，これらの検討課題を解決するために，Fig. 2 に示すように 4 つの項目を中心に研究を行ってきた．これらの項目の中で，*in vivo* 研究については，比較的研究初期の段階から中心的に取り組んできた．その中で，繊維

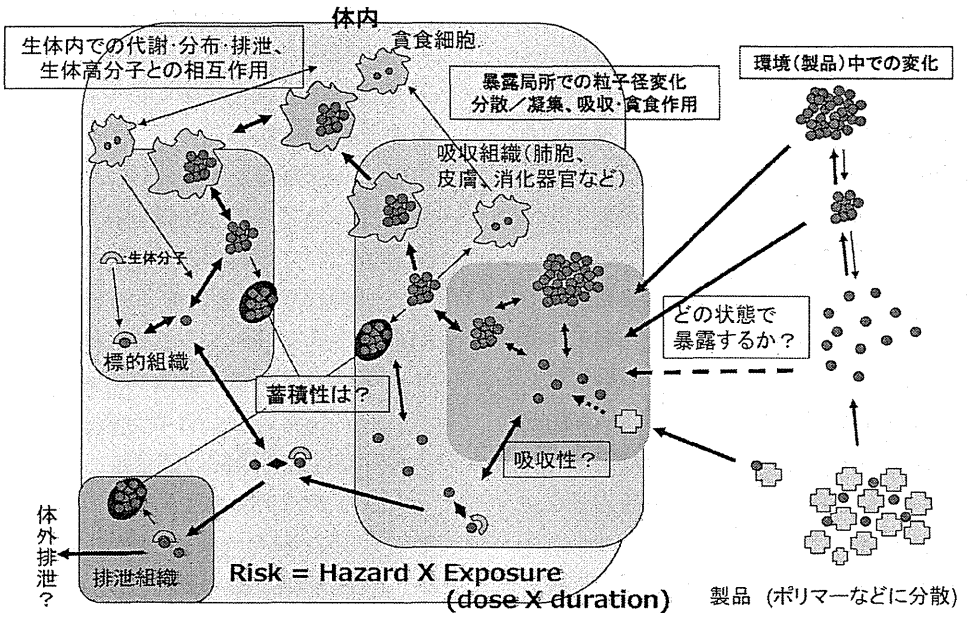

Fig. 1. The Estimated ADME Schema of Nanomaterials

***in vivo*試験法研究**

MWCNTのP53ヘテロ欠失マウスへのi.p.投与による中皮腫誘発性を確認
バイオマーカとしてマウスのメソセリン抗体の作成
一方、C60の腹腔内投与による慢性的影響として腎臓への影響を示唆
TiO_2と C60の気管内投与による発がんプロモーション作用の示唆

吸入試験法研究

MWCNTのミスト暴露システムを開発
気管内投与時の分散性依存の発現様式差異を確認
リポソーム分散C60による気管内投与法を開発。

暴露測定法／動態解析研究

生体試料でのC60の定量的検出法との確立
静注後のC60の組織からの経時的消失検討
気管内投与後のMWCNTの肺及び肝臓での検出

***in vitro*試験法研究**

細胞培養系でのリポソーム等を用いた分散法の確立
→C60やTiO_2の遺伝毒性、細胞透過性、
神経系の細胞機能への影響、などへの適用

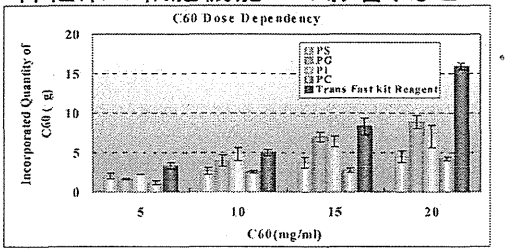

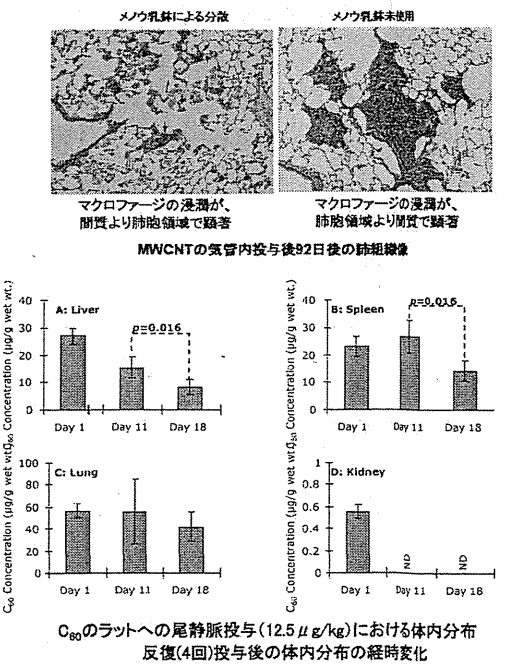

C_{60}のラットへの尾静脈投与（12.5 μg/kg）における体内分布
反復(4回)投与後の体内分布の経時変化

Fig. 2. The Overall Results of NIHS Projects for Nanomaterial Safety

長の長いタイプの多層型カーボンナノチューブ（MWCNT）が，中皮腫を誘発する可能性を持つことを確認した.[6] 上記の体内動態の重要性を考慮した概念からは，吸収性や体内分布について検証したのちに，慢性影響の可能性を検討することが論理的であるが，研究開始当時から，大量生産可能であった，酸化チタン（TiO_2）やフラーレン（C60），MWCNTについては，*in vivo* の慢性影響を先行して検討しておくべきであると判断した．特にその形状がアスベストに似ていたMWCNTについては，吸入曝露による有害影響が懸念されたが，MWCNTについての吸入曝露法が確立していない段階では，アスベストでも検証に使用されていた腹腔内投与による中皮腫誘発試験を行うこととした．

われわれの最初の実験は，アスベストで中皮腫の誘発時期が早くなることが知られているp53ヘテロノックアウトマウスへの腹腔内へ3 mg/mouseという高用量を投与することによって確認されたものであり，動物種の特異性や投与量の多さについて異論も指摘された．しかしその後の研究で，野生型の動物種であるF344ラットに対しても，同じMWCNTが中皮腫の誘発作用を持つことが確認された[7]ほか，投与量を1000分の1にまで少なくした実験においても中皮腫の起きることが示されている（投稿中）．

酸化チタンについては，雌ラットへの吸入曝露により発がん性のあることが示されているが，ナノサイズ化による発がん性の検証のために，気管内投与による肺がんのプロモーション作用の検討を行った．その結果，酸化チタンは，肺腺腫や乳腺腫に対してプロモーション作用を示し，その作用は，マクロファージから放出される炎症性因子であるMIP1αを介したものであることが示唆された.[8] 現在C60やMWCNTを用いたプロモーション作用の検討が進行中である．

一方，曝露手法の開発においては，ミスト法や粉体法によるMWCNTの吸入曝露システムの開発研究を進めているが，より簡易な手法として気管内投与のための適切な分散法の検討を行った．その結果，分散法の違いが肺の有害性発現様式に違いを引き起こすことを確認した.[9]

体内動態解析のために，生体試料中のC60やTiO_2の分析手法の開発や改良を行い，経口投与や気管内投与による体内吸収性について検討を行っている．現在のところ投与部位である消化管や肺以外で有意な検出量を確認できておらず，感度の向上に向けた研究を進めている．しかし，体内への吸収を前提にした解析として，C60の静脈内投与による解析を行ったところ，肝臓や脾臓，肺などへの分布を確認したが，腎臓への分布は極めて低いことが示された（投稿中）．その他，遺伝毒性や標的臓器などの毒性をスクリーニングするための *in vitro* 試験における培地等への分散法も検討対象としており，リポソームを用いたC60の分散法を確立した．

4. 慢性影響研究の重要性

ナノマテリアルの生体影響に関する情報はここ数年の活発な研究状況を反映して多くなりつつあるが，慢性影響に関する報告は依然その数が少ない状況である．一般の化学物質の有害性評価の常套手段として，変異原性試験や短期試験から情報を収集していくことは，必要なステップであり，OECDにおけるナノマテリアル作業グループの活動におけるスポンサーシッププログラムにおいても，加盟各国からの毒性試験情報として，短期試験を中心に収集されてきている．われわれの研究グループにおいても，これらの枠組みに対して，短期的な試験情報を中心に提供し始めている段階である．しかしMWCNTに関しては，研究初期から，短期毒性より長期毒性の方が懸念の強いことが，物性等の情報から推測されたところでもあり，その推定に基づいて，腹腔内投与の研究を最初にスタートさせた．腹腔内投与は，リスク評価の観点からは，曝露経路（吸入曝露）に伴う定量的な評価に問題のあるところであるが，最近の注目すべき研究として，分散剤で分散させたMWCNT（最高80 μgまで）をマウスに吸引させた研究や，MWCNT: 30 mg/m^{3}をマウスに単回吸入曝露した研究において，曝露後7-8週間目にMWCNTが胸膜に到達していたことが報告されている.[10,11] これらの研究結果は高用量の曝露による短期間の結果ではあるが，呼吸器を経由した曝露においてもMWCNTは胸膜（中皮）まで到達することを示唆しており，われわれの腹腔内投与による結果と合わせると，リスク評価の上でも重要な知見であると考えられる．

これらの腹腔内投与による中皮腫誘発能は，繊維状粒子による催腫瘍性のみを検出する系であり，短

いタイプやその他様々な形状の MWCNT における慢性毒性は別途検証する必要性がある．実際，われわれの行った腹腔内投与試験では，小さいサイズのナノチューブ繊維を含んだ細胞が腹膜の病変部のみならず，肝類洞内，又は肝葉間や腸間膜リンパ節の中にも認められ，体内に再分布することが示唆された（Fig. 3）.[6] さらに，SWCNT をマウスへ咽頭吸引させた実験では，一過性の急性症状の後に，炎症性細胞浸潤を伴わない間質の繊維化が認められている.[12] また，ApoE ノックアウトマウスを用いた実験では，タンパクカルボニル化活性の変化を伴うミトコンドリア DNA 障害と，アテローム性動脈硬化症の進行を増強することが示された.[13] MWCNT に関しても，マウスに MWCNT（200–400 μg）を気管内滴下した実験では，一過性の肺の炎症反応に加え，投与量に依存した血小板の活性化と凝固作用の活性化の促進が示唆されている.[14] また，MWCNT や SWCNT の気管内投与や経鼻投与により，アレルギー反応の増強反応が報告されている.[15–17] これらの結果が，カーボンナノチューブが直接体内循環に侵入した結果であるか，免疫細胞との接触を介した反応であるかを区別することは難しいが，曝露局所に留まらない全身作用の可能性を示している．われわれの酸化チタンの気管内投与による発がんプロモーション作用が，炎症因子により介在されたことは，これらの知見と同様の作用様式を示すものととらえることもできる．

以上の知見は，短期の試験だけでは検証することは困難であり，ナノマテリアルの有害性を確認するためには，長期の体内動態予測や慢性影響に関する研究が，重要なステップであることを示している．Figure 4 にスクリーニング試験や確定試験を開発するための手順についてまとめた．通常の化学物質については，その長い歴史の中で明らかとなった有害性に対して，それぞれの毒性発現様式に応じてスクリーニング試験が開発され，現在まで運用されてきている．特に変異原性試験は発がん性を予測する試験としての重要な役割を担っている．しかし，現時点ではナノマテリアルによる有害性影響が，これまでの研究経験の中で明らかとなった影響だけに留まるのかについては，まだ誰も判定できない状況である．これまでの一般化学物質に対応する有害性とスクリーニング試験を活用して進めていくと同時に，未知の影響を見極める最初のステップとして，少な

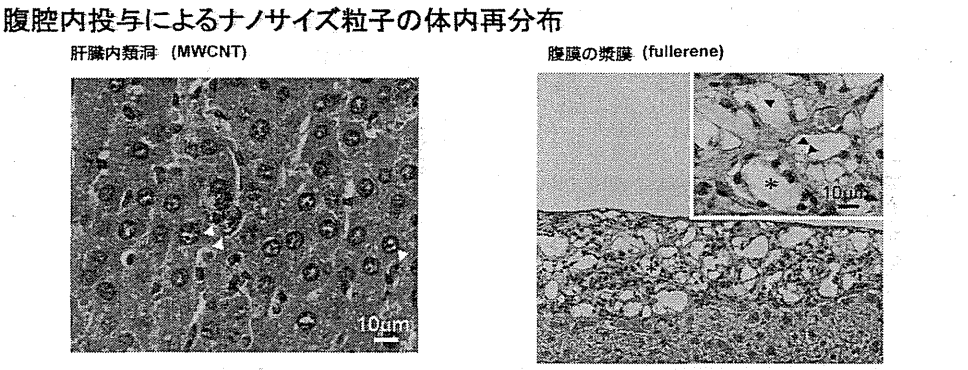

A. Takagi et al., J. Toxicol. Scie., **33**,105-116. (2008)

SWCNTやMWCNTによる全身性影響の示唆

- アテローム性動脈硬化症の進行の増強の可能性（ApoE$^{-/-}$マウス）
  Z. Li *et al.*, *Environmental health perspectives*. **115**, 377-382 (2007)
- 血小板の活性化と凝固作用の活性化（MWCNT気管内滴下）
  A. Nemmar *et al.*, *J. Thrombosis, Haemostasis* **5:** 1217-1226 (2007)
- アレルギー反応の増強（MWCNT・SWCNT、気管内・経鼻投与）
  E.J. Park *et al.*, *Toxicology*. **259**, 113-21 (2009)
  U.C. Nygaard *et al.*, *Toxicol Sci.* **109**, 113-23 (2009)
  K. Inoue *et al.*, *Toxicol Appl Pharmacol.* **237**, 306-16 (2009)

Fig. 3. The Suggestive Evidences for Systemic Toxicites by Nanomaterials

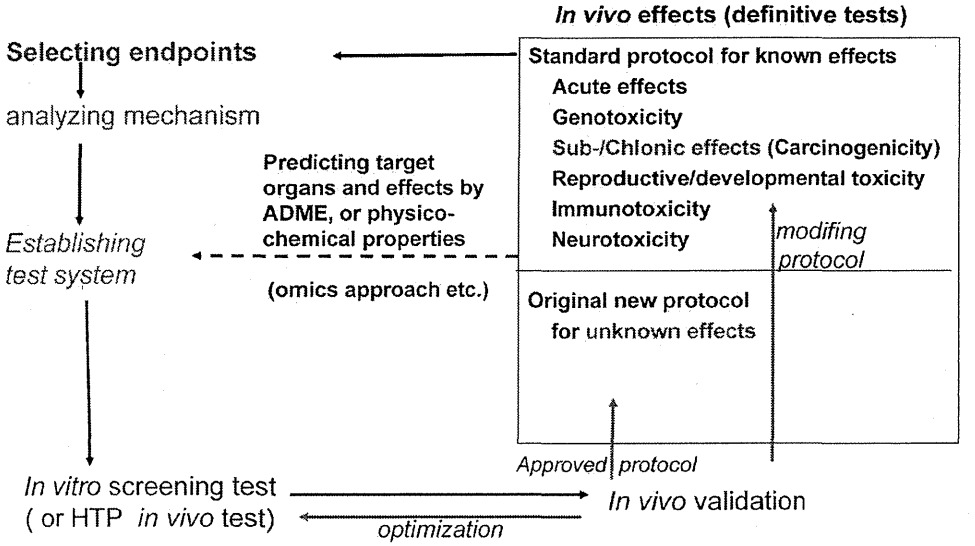

Fig. 4. The Schematic Development of Screening Tests and Definitive Tests

くとも代表的なナノマテリアルによる *in vivo* の慢性影響研究や，その影響を推定するためのナノマテリアルと生体成分との分子レベルでの相互作用や体内残留性様式の解析を進めていくべきであると考えられる.

謝辞 本稿で解説した研究成果の一部は，厚生労働科学研究費補助金（化学物質リスク研究事業）H17-化学-012，H18-化学--一般-007 及び H21-化学--一般-008 の助成によって行われたものです.

REFERENCES

1) Scientific Committee on Emerging and Newly Identified Health Risks, SCENIHR: ⟨http://ec.europa.eu/health/ph_risk/committees/04_scenihr/docs/scenihr_o_003b.pdf⟩, European Commission Web, cited 14 November, 2010.
2) Scientific Committee on Emerging and Newly Identified Health Risks, SCENIHR: ⟨http://ec.europa.eu/health/ph_risk/committees/04_scenihr/docs/scenihr_o_010.pdf⟩, European Commission Web, cited 14 November, 2010.
3) Food Safety Authority of Ireland, FSA, "The Relevance for Food Safety of Applications of Nanotechnology in Food and Feed Industries," Dublin, 2008.
4) UK Committees on Toxicity, Mutagenicity and Carcinogenicity of Chemicals in Food, Consumer Products and the Environment (COT, COM, COC): ⟨http://cot.food.gov.uk/pdfs/cotstatements2005nanomats.pdf⟩, COT Web, cited 14 November, 2010.
5) The Committee on Toxicity of Chemicals in Food, Consumer Products and the Environment: ⟨http://www.food.gov.uk/multimedia/pdfs/cotstatementnanomats200701.pdf⟩, cited 14 November, 2010.
6) Takagi A., Hirose A., Nishimura T., Fukumori N., Ogata A., Ohashi N., Kitajima S., Kanno J., *J. Toxicol. Sci.*, **33**, 105-116 (2008).
7) Sakamoto Y., Nakae D., Fukumori N., Tayama K., Maekawa A., Imai K., Hirose A., Nishimura T., Ohashi N., Ogata A., *J. Toxicol. Sci.*, **34**, 65-76 (2009).
8) Xu J., Futakuchi M., Iigo M., Fukamachi K., Alexander D. B., Shimizu H., Sakai Y., Tamano S., Furukawa F., Uchino T., Tokunaga H., Nishimura T., Hirose A., Kanno J., Tsuda H., *Carcinogenesis*, **31**, 927-935 (2010).
9) Wako K., Kotani Y., Hirose A., Doi T., Hamada S., *J. Toxicol. Sci.*, **35**, 437-446 (2010).
10) Nurkiewicz T. R., Porter D. W., Hubbs A. F., Stone S., Chen B. T., Frazer D. G., Boegehold M. A., Castranova V., *Toxicol. Sci.*, **110**, 191-203 (2009).
11) Ryman-Rasmussen J. P., Cesta M. F., Brody

A. R., Shipley-Phillips J. K., Everitt J. I., Tewksbury E. W., Moss O.R., Wrong B. A., Dodd D. F., Andersen M. E., Bonner J. C., *Nat. Nanotechnol.*, **4**, 747–751 (2009).

12) Shvedova A. A., Kishin E. R., Mercer R., Murray A. R., Johnson V. J., Potapovich A. I., Tyurina Y. Y., Gorelik O., Arepalli S., Schwegler-Berry D., Hubbs A. F., Antonini J., Evans D. E., Ku B. K., Ramsey D., Maynard A., Kagan V. E., Castranova V., Baron P., *Am. J. Physiol. Lung cell. mol. physiol.*, **289**, L698–L708 (2005).

13) Li Z., Hulderman T., Salmen R., Chapman R., Leonars S. S., Young S. H., Shvedova A., Luster M. I., Simeonove P. P., *Environ. Health Perspect.*, **115**, 377–382 (2007).

14) Nemmar A., Hoet P. H., Vandervoort P., Dinsdale D., Nemery B., Hoylaerts M. F., *J. Thromb. Haemost.*, **5**, 1217–1226 (2007).

15) Park E. J., Cho W. S., Jeong J., Yi J., Choi K., Park K., *Toxicology*, **259**, 113–121 (2009).

16) Nygaard U. C., Hansen J. S., Samuelsen M., Alberg T., Marioara C. D., Løvik M., *Toxicol. Sci.*, **109**, 113–123 (2009).

17) Inoue K., Koike E., Yanagisawa R., Hirano S., Nishikwa M., Takano H., *Toxicol. Appl. Pharmacol.*, **237**, 306–316 (2009).

The Journal of Toxicological Sciences (J. Toxicol. Sci.)
Vol.37, No.1, 177-189, 2012

Original Article

Effects of sustained stimulation with multi-wall carbon nanotubes on immune and inflammatory responses in mice

Atsumi Yamaguchi[1], Tomoko Fujitani[1], Ken-ichi Ohyama[1], Dai Nakae[2], Akihiko Hirose[3], Tetsuji Nishimura[4], Akio Ogata[1]

[1]Departments of Environmental Health and Toxicology and [2]Departments of Pharmaceutical Sciences, Tokyo Metropolitan Institute of Public Health, 3-24-1 Hyakunin-cho, Shinjuku-ku, Tokyo 169-0073, Japan
[3]Divisions of Risk Assessment and [4]Divisions of Environmental Chemistry, National Institute of Health Science, 1-18-1 Kamiyoga, Setagaya-ku, Tokyo 158-8501, Japan

(Received October 19, 2011; Accepted December 5, 2011)

ABSTRACT — Possible effects of multi-wall carbon nanotubes (MWCNTs) on immune and inflammatory responses were examined in mice. Female ICR mice were given a single intraperitoneal administration (2 mg/kg body weight) of either MWCNTs, carbon black (CB), or crocidolite (blue asbestos) and controls received a vehicle of 2% sodium carboxymethyl cellulose (CMC Na). In the peritoneal cavity of MWCNT-administered mice, the liver had changed to a rounded shape and fibrous adhesions were seen on internal organs. Peritoneal cells overexpressed mRNA for genes of T helper (Th)2 cytokines (*interleukin [IL]-4*, *IL-5*, and *IL-13*), Th17 cytokine (*IL-17*), pro-inflammatory cytokines/chemokines (*IL-1β*, *IL-33*, *tumor necrosis factor α*, and *monocyte chemotactic protein-1*), and *myeloid differentiation factor 88* for at least 2 weeks after the administration of MWCNTs, while those of Th1 cytokine genes (*IL-2* and *interferon γ*) were overexpressed several weeks later and expression levels remained high up to 20 weeks. In MWCNT-treated mice, the numbers of leukocytes, monocytes, and granulocytes in the peripheral blood and the expression of the leukocyte adhesion molecules, cluster of differentiation (CD)49d and CD54, on granulocytes were increased 1 week after administration and remained high up to week 20. Production of ovalbumin-specific IgM and IgG_1 was enhanced by MWCNTs. These changes were not observed after CB or crocidolite administration. Thus, this study showed that MWCNTs exhibited sustained stimulating effects on immune and inflammatory responses, unlike the other mineral fibers with structural similarities.

Key words: Multi-wall carbon nanotube, Nanomaterial, Inflammation, Immunotoxicity, Hazard characterization

INTRODUCTION

Rapid progress in nanotechnology in recent years has made it possible to produce and apply numerous new and useful nanomaterials, such as nano-TiO_2, nano-SiO_2, nano-ZnO and nano-carbon materials. These are believed to be biologically inert, although inhalation of small-sized nanomaterials can cause pulmonary inflammation and fibrosis. (Mossman and Churg, 1998; Yazdi *et al.*, 2010). Carbon forms exist in many different shapes as both elementary substances and compounds, for example, diamond, charcoal, carbon black, graphite, fullerene, and carbon nanotubes are all carbon allotropes, while graphene is a single-wall product of graphite, whose structure consists of one-atom-thick planar sheets of hexagonal-bonded carbon atoms densely packed in honeycomb crystal lattices. Carbon nanotubes are seamless cylindrical structures comprising single or multiple graphene sheets. Both single-wall carbon nanotubes (SWCNTs) and multi-wall carbon nanotubes (MWCNTs) are several micrometers in length and approximately 1-20 nanometers in diameter. These needle-like structures resemble asbestos.

It is well known that asbestos inhalation causes pulmonary inflammation and fibrosis, lung cancer, and malignant mesothelioma after relatively long latency periods (Mossman *et al.*, 1990; Hei *et al.*, 1992). However, the signaling pathways that lead to the development of these asbestos-associated diseases remain largely unknown. If

Correspondence: Atsumi Yamaguchi (E-mail: Yamaguchi@member.metro.tokyo.jp)

carbon nanotubes can create the hazards and risks similar to those associated with asbestos, they must be appropriately assessed and managed to protect human health.

In vivo effects of MWCNTs have been studied using animal models with a variety of exposure methods, such as inhalation, intratracheal instillation, pharyngeal aspiration, and intraperitoneal injection, and their effects on inflammatory responses have been described. Mice exposed to MWCNTs by inhalation caused platelet-derived growth factor (PDGF) overexpression, inflammatory cell aggregation, and recruitment of macrophages that phagocytosed MWCNTs in the lung within 1 day, followed by the subsequent development of subpleural fibrosis during weeks 2-6 (Ryman-Rasmussen *et al.*, 2009a, 2009b). Pharyngeal aspiration of MWCNTs in mice caused the rapid development of fibrosis within 7 days and a persistent granulomatous inflammation throughout a 56-day post-exposure period (Porter *et al.*, 2010). Intratracheal instillation of MWCNTs in mice caused an increase in the number of neutrophils and the levels of cytokines in bronchoalveolar lavage (BAL) fluid within 1 day, and granulomatous lesions developed and persisted until day 14 of these experiments (Park *et al.*, 2009). Intraperitoneal injection of MWCNTs given to rats (Sakamoto *et al.*, 2009) or *p53* gene heterozygously deficient mice (Takagi *et al.*, 2008) induced a long-lasting inflammation and resulted in fibrous thickening and granuloma formation in the peritoneum in association with the induction of mesothelioma.

However, despite evidences from these studies, the potential immunotoxicity of MWCNTs has not been sufficiently established till date. Thus, the present study was conducted to assess a possible involvement of MWCNTs in immune and inflammatory responses of ICR mice. Intraperitoneal administration was chosen as the exposure route for MWCNTs. Although it may not be directly relevant to humans, intraperitoneal administration in a rodent model is sensitive enough to detect weak effects of MWCNTs, which was why this strategy was adopted to identify a possible carcinogenic hazard of MWCNTs (Sakamoto *et al.*, 2009; Takagi *et al.*, 2008). In addition, intraperitoneal administration can control and ensure the relationship between administration doses and agent exposure. Furthermore, some reports have clearly indicated the detection of inhaled MWCNTs in the subpleura (Ryman-Rasmussen *et al.*, 2009a), pharyngeally-aspirated MWCNTs in the pleura (Porter *et al.*, 2010), and intraperitoneally-administered MWCNTs in the liver and mesenteric lymph nodes (Sakamoto *et al.*, 2009). These results suggest that MWCNTs are distributed to a certain extent in the entire body, regardless of the exposure route used.

MATERIALS AND METHODS

Ethical approval

Our experimental protocols were approved by the Experiments Regulation Committee and the Animal Experiment Committee of the Tokyo Metropolitan Institute of Public Health prior to beginning of these experiments and were monitored at each step of experimentation for scientific and ethical appropriateness, including concerns for animal welfare, with strict adherence to the National Institutes of Health Guidelines for the Care and Use of Laboratory Animals, Japanese Government Animal Protection and Management Law, Japanese Government Notification on Feeding and Safekeeping of Animals, and other similar laws, guidelines, and rules provided domestically and internationally.

Animals

Specific pathogen-free female Crlj:CD1(ICR) mice, 6-7 weeks old, were purchased from Charles River Japan, Inc. (Kanagawa, Japan) and acclimatized for 1 week. Mice were housed individually in plastic cages (22 × 15 × 12 cm) with cedar chip bedding and had free access to a standard diet CE2 (Nihon Clea, Inc., Tokyo, Japan) and water. The animal room was maintained at 24°C-26°C with a relative humidity of 50%-60%, with 10 ventilations per hour (drawing fresh air through a high-efficiency particulate air filter, 0.3 μm, 99.9% efficiency), and on a 12 hr light/dark cycle.

Chemicals, reagents, and kits

MWCNTs (MITSUI MWCNT-7; lot number 060125-01k) were provided by National Institute of Health Science, Tokyo, Japan. These were exactly identical to those used in carcinogenicity studies with male Fisher 344 rats (Sakamoto *et al.*, 2009) and male C57BL/6-originated mice that were heterozygously deficient in the *p53* gene (Takagi *et al.*, 2008); these reports describe their physicochemical properties. Carbon black (CB; 22 nm in diameter) was purchased from Showa Chemical Industry Co., Ltd. (Tokyo, Japan). UICC-grade crocidolite was provided by the Tokyo Metropolitan Institute of Public Health.

Ovalbumin (OVA) and bovine serum albumin (BSA) were purchased from Sigma-Aldrich Co. (St. Louis, MO, USA). Horseradish peroxidase (HRP)-conjugated anti-mouse IgM and IgG_1 antibodies were purchased from Zymed Laboratories (South San Francisco, CA, USA). 2,2'-Azino-bis(3-ethylbenzothiazoline-6-sulfonic acid) diammonium salt (ABTS) tablets, a substrate for HPR-conjugated antibodies, were purchased from Roche

Diagnostics Division (Basel, Switzerland). Monoclonal anti-OVA-IgG_1 antibody (clone OVA-14) was purchased from Sigma-Aldrich. Phycoerythrin-conjugated (PE-) anti-CD3 (derived from T cell clone 145-2C11), fluorescein isothiocyanate-conjugated (FITC-) anti-CD45R (B220) (derived from B cell clone RA3-6B2), PE- anti-CD8 (clone 53-6.7), and FITC- anti-CD4 (clone GK1.5) were purchased from Beckman Coulter, Inc. (Fullerton, CA, USA). PE-Cy5.5--anti-CD3 (clone 145-2C11), PE-Cy5.5--anti-CD45 (derived from leukocyte clone 30-F11), PE--anti-CD14 (derived from monocyte clone: Sa2-8), PE--anti-Ly-6G (derived from granulocyte clone RB6-8C5), FITC--anti-CD54 (intercellular adhesion molecule [ICAM]-1; clone YN1/1.7.4), FITC--anti-CD49d (integrin α4; clone R1-2), FITC-anti-CD11b (integrin αM; clone 1/70), and anti-CD16/CD32 (Fcγ receptor III/II; clone 93) antibodies were purchased from eBioscience, Inc. (San Diego, CA, USA). RNAprotect Cell Reagent, RNeasy Mini kit, High Capacity RNA-to-cDNA kit, TaqMan Gene Expression Master Mix, and TaqMan Gene Expression Assays Inventoried were purchased from Life Technologies Co. (Carlsbad, CA, USA).

Animal experiments

Three independent animal experiments were conducted; protocols for handling test chemicals were identical in each. MWCNTs, CB, or crocidolite was suspended in 2% sodium carboxymethyl cellulose (CMC Na) to a concentration of 0.2 mg/ml. A single intraperitoneal dose (2 mg/kg body weight) of each of these was administered to mice. In a vehicle control group, CMC Na was administered with a single intraperitoneal volume of 10 ml/kg body weight.

The first animal experiment included histopathological examination and real-time polymerase chain reaction (PCR) assays for mRNA expression of cytokine/chemokine genes. Within 32 weeks, 2 of 6 mice that were administered MWCNT died; hence, the last experiment was conducted at the end of 34 weeks after administration. Mice were maintained up to 34 weeks after their exposure to test chemicals or vehicle. From each treatment or vehicle group, 3-6 animals were chosen for assays at the end of 2, 4, 10, 20, and 34 weeks. Under light ether anesthesia, cells were collected from the abdominal cavity and suspended in 5 ml of phosphate-buffered saline (PBS), centrifuged at 1,200 rpm for 10 min, and stored in RNAprotect Cell Reagent until RNA extraction for the real-time PCR assay. Tissues and organs were harvested for histopathological examinations. Samples were fixed in neutrally buffered formalin, embedded in paraffin, and stained with sirius red for collagen or hematoxylin-eosin.

The second animal experiment included flow cytometry analysis of the peripheral blood cells. Mice were maintained up to 20 weeks after their exposure to test chemicals or vehicle. From each treatment or vehicle group, 4 animals were chosen for the assays on day 2 and at the end of 1, 2, 4, and 20 weeks. Under light ether anesthesia, approximately 1 ml of blood was collected through cardiac puncture into a syringe with 20 μl of an anticoagulant, ethylenediaminetetraacetic acid, and used for flow cytometry.

The third animal experiment included determinations of OVA-specific immunoglobulins. After their exposure to test chemicals or vehicle, mice were immunized with OVA/alum intraperitoneally administered at a dose of 100 μg/mouse on days 2 and 10 as previously described (Ito *et al.*, 2002). Under light ether anesthesia, blood samples of approximately 0.1 ml were collected from a tail vein. Samples were taken from 10 to19 animals from each treatment or vehicle group from the tail vein 8 days after the last immunization for IgM and from 15 animals from each group 20 days after the last immunization for IgG_1. Serum was stored at -80°C until assayed.

Real-time PCR assays for mRNA expression of cytokine/chemokine gene

Total RNA was isolated from 5 x 10^4 peritoneal cells obtained in the first animal experiment as described above, using RNeasy Mini kit. RNA from untreated 8-16-week-old female ICR mice were prepared separately, pooled, and used as a basal expression control. First-strand cDNA was prepared from 0.9 μg of RNA using a High Capacity RNA-to-cDNA kit. PCR used TaqMan Gene Expression Master Mix for genes (*IL-1β*, Mm01336189_m1; *IL-2*, Mm00434256_m1; *IL-4*, Mm99999154_m1; *IL-5*, Mm99999063_m1; *IL-6*, Mm99999064_m1; *IL-8*, Mm00436450_m1; *IL-10*, Mm99999062_m1; *IL-13*, Mm00434204_m1; *IL-17*, Mm00439619_m1; *IL-18*, Mm00434225_m1; *IL-33*, Mm00505403_m1; *IFNγ*, Mm99999071_m1; *MCP-1*, Mm00441242_m1; *MyD88*, Mm00440338_m1; *TGFβ1*, Mm03024053_m1; *TNFα*, Mm99999068_m1; *TATA box binding protein [TBP]*, Mm00446973_m1; *hypoxanthine phosphoribosyltransferase [HPRT]*, Mm00446968_m1), cDNA-specific TaqMan Gene Expression Assays, and an ABI 7500 Real-Time PCR System (Life Technologies). All PCR reactions were performed in duplicates. The quantity of PCR product was determined by the Comparative Ct Method as described by the manufacturer, in which each sample was normalized against the value of a housekeeping gene, *HPRT*. Fold-changes were expressed as either an increase or decrease compared with the basal expression control level.

Flow cytometry analysis of the peripheral blood cells

After 15 minute pre-incubation with an anti-CD16/32 monoclonal antibody to prevent non-specific binding, a peripheral blood sample (100 μl) obtained in the second animal experiment described above was reacted with various combinations of antibodies. After a 30-min incubation in the dark, erythrocytes were lysed with 4 ml of Tris (1 g/500 ml)plus NH_4Cl (2.8 g /500 ml) for 10 min, suspended in 4 ml of PBS, and centrifuged at 1,200 rpm for 10 min. The cell pellet was washed in PBS with 0.5% BSA. Fluorescence intensity and cell numbers were determined using a Cell Lab Quanta SC (Beckman Coulter). The number of leucocytes was counted as positive cells of PE-Cy5.5- anti-CD45 antibody. The number of lymphocytes was distinguished based on CD45 fluorescence and side scatter. T and B cells were distinguished based on PE and FITC fluorescence from PE-Cy5.5- CD45 positive cells. CD4 and CD8 cells were distinguished based on PE and FITC fluorescence from PE-Cy5.5- CD3 positive cells. Percent of CD11b, CD49d, and CD54 positive cells was measured based on FITC fluorescence from CD45 and CD14 or CD45 and Ly6G positive cells.

Serum OVA-specific immunoglobulin concentrations

Concentrations of OVA-specific IgM and IgG_1 in serum were determined using ELISA. We added 100 μl of 100 μg/ml of OVA to wells of a microtest plate and incubated the plates overnight at 4°C. Wells were washed 6 times with 0.05% Tween20/PBS (0.05T/PBS) and blocked with 5% BSA in PBS (5B/PBS) for 2 hr at room temperature. Diluted serum (IgM: 1/150, IgG_1: 1/5 x 10^6) was then added to each well and incubated for 2 hr. After 6 washes with 0.05T/PBS, the wells were blocked with 5B/PBS for 1 hr at room temperature. HRP-labeled anti-mouse IgM and IgG_1 antibodies were added to each well, and the plates were incubated for 2 hr at room temperature. After 6 washes with 0.05T/PBS, a substrate solution prepared using ABTS Tablets according to the manufacturer's instructions was added and the color reaction was allowed to develop in the dark at room temperature for 30 min. Optical density (OD) at 405 against 492 nm was determined using a microplate reader (SUNRISE REMOTE; Wako Pure Chemical Industries, Ltd., Osaka, Japan). Values for anti-OVA antibody were used as basal expression control.

Statistical analysis

Intergroup comparisons were made using Student's *t*-test. Significance level was set at p value < 0.05 .

RESULTS

General findings

During the course of the experiments, the body weights of mice increased within the same range after intraperitoneal administration of CMC Na, MWCNTs, CB, or crocidolite. In the first animal experiment, morphological assessments were conducted for mice that were given a single intraperitoneal administration of MWCNT, CB, or crocidolite. In the abdominal cavities of MWCNT-treated mice as compared with CMC Na-treated mice, liver edges had lost their sharpness, fibrous adhesions were seen on internal organs, and deposits were observed on the surfaces of the liver and diaphragm (Figs. 1a and 1b). In CB-treated mice, deposits were scattered in the abdominal cavity, especially on intestinal surfaces (Fig. 1c). No noteworthy changes were observed in the abdominal cavities of the CMC Na- or crocidolite-treated mice (Figs. 1a and 1d), or anywhere outside of the abdominal cavity in any of the groups.

Peritoneal cells obtained from MWCNT-treated mice contained small amounts of erythrocytes as compared with CMC Na-treated mice (Figs. 2a and 2b), whereas numerous erythrocytes were found for the crocidolite-treated mice (Fig. 2d). The peritoneal cells obtained from the CB-treated mice looked black, presumably because of the engulfment of the test chemical (Fig. 2c).

Fig. 3 showed the micrograms of liver, and Fig. 3a and 3b were the liver of CMC Na treated-mice that had thin layered mesothelium. Histopathological examinations revealed that the hepatic visceral peritoneum had fibrous thickening along with mesothelial cell hypertrophy in the MWCNT-treated mice (Figs. 3c and 3d). Inflammatory cells had infiltrated into this fibrously thickened visceral peritoneum. The majority of these infiltrating cells were macrophages containing MWCNTs, along with eosinophils, plasma cells, and immature myeloid cells (Fig. 3e) that occasionally formed a granulation (Fig. 3c). These changes were not observed in the CB- or crocidolite-treated mice.

No tumorigenic changes were observed either macroscopically or histopathologically in any of the mice treated with any of the test chemicals within the 34-week experimental period.

Expression of cytokine mRNA in peritoneal cells

mRNA expression levels of certain cytokine genes were substantially increased in the peritoneal cells obtained from MWCNT-treated mice, and these high levels were maintained up to the ends of 20 and 34 weeks. Th2 cytokine gene mRNA levels for *IL-4*, *IL-5*, and *IL-13*

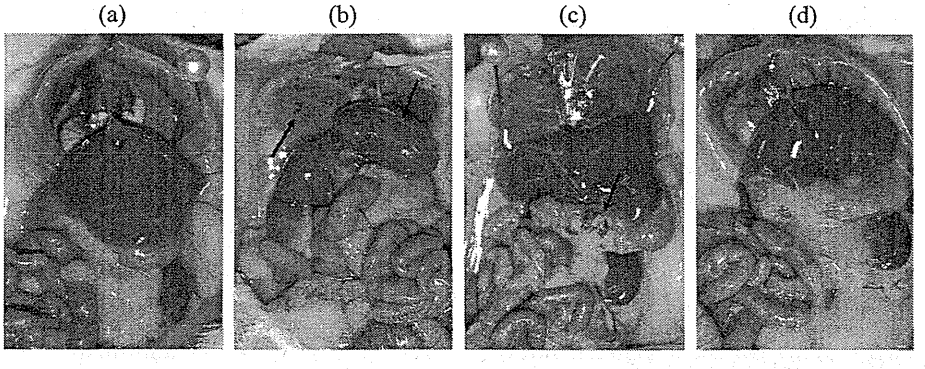

Fig. 1. Representative macroscopic appearances of the mouse abdominal cavity in the first animal experiment. Observations were made at 10 weeks after exposure to (a) CMC Na, (b) MWCNTs, (c) CB, or (d) crocidolite. Arrows indicate deposits of test chemicals.

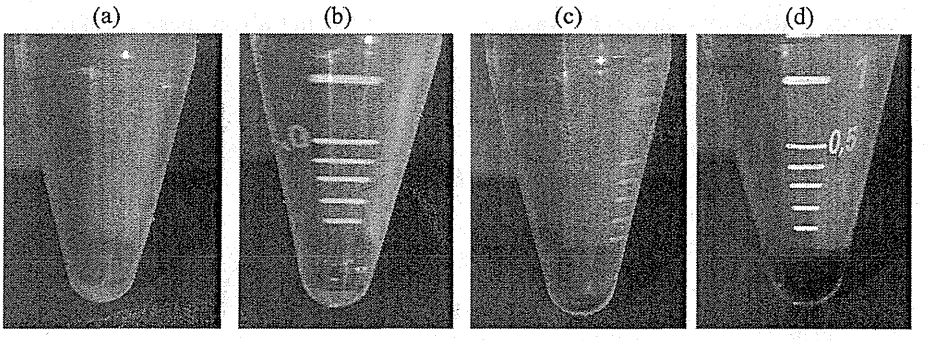

Fig. 2. Representative macroscopic appearances of peritoneal cells obtained from mice in the first animal experiment. Observations were made at 10 weeks after exposure to (a) CMC Na, (b) MWCNTs, (c) CB, or (d) crocidolite.

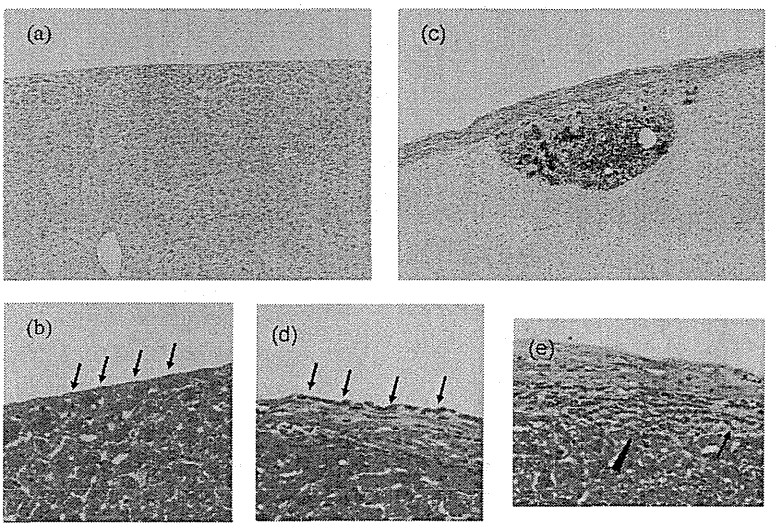

Fig. 3. Representative histology of the mouse liver in the first animal experiment. Examinations were made at 20 weeks after exposure to (a, b) CMC Na or (c-e) MWCNTs. Arrows indicate mesothelial cells and arrowheads indicate the infiltrations of eosinophils and immature myeloid cells. (a) and (c) were stained with sirius red staining, x 100, and (b), (d), and (e) were stained with hematoxylin-eosin, x 400.

were significantly increased from 2 to 20 weeks after administering MWCNTs. When compared with the basal expression control value for untreated animals, mRNA levels of *IL-4* were 34, 43, 24, 60, and 3 times higher, those of *IL-5* were 110, 127, 63, 226, and 69 times higher, and those of *IL-13* were 55, 38, 11, 28, and 3 times higher at 2, 4, 10, 20, and 34 weeks, respectively, after administering MWCNTs (Fig. 4).

Overexpression of mRNA of Th1 cytokine genes, *IL-2* and *IFNγ*, were delayed compared with mRNA of Th2 cytokine genes, but were also sustained; however, these were not significantly higher than basal expression levels except for *IL-2* at the end of 34 weeks. mRNA expression levels of *IL-2* were 0.3, 0.6, 1.5, 5.4, and 4.8 times higher, and those of *IFNγ* were 0.5, 0.3, 0.6, 1.6, and 4.3 times higher at the end of 2, 4, 10, 20, and 34 weeks, respectively (Fig. 4). Sustained mRNA overexpression was also found for a Th17 cytokine gene, *IL-17*, and these increases were significant at the end of 10 to 20 weeks.

mRNA for genes of proinflammatory cytokines, *IL-1β*, *IL-33*, and *TNFα*, and an inflammatory chemokine, *MCP-1*, were increased significantly at the end of 2 to 20 weeks (*IL-1β* and *TNFα*) and at 2 to 34 weeks (*IL-33* and *MCP-1*). mRNA level of an adapter protein of Toll-like receptors (TLR), *MyD88*, was also increased significantly at the end of week 2 to 20. mRNA levels of *IL-17* were 9, 13, 9, 26, and 25 times higher, those of *IL-1β* were 29, 23, 32, 28, and 19 times higher, those of *IL-33* were 13, 20, 5, 13, and 20 times higher, those of *TNFα* were 3, 2, 2, 3, and 2 times higher, those of *MCP-1* were 17, 28, 41, 49, and 42 times higher, and those of *MyD88* were 3, 3, 2, 2, and 1 time higher at 2, 4, 10, 20, and 34 weeks, respectively, after MWCNT administration (Figs. 4 and 5). mRNA levels of other inflammatory cytokine genes (*IL-6*, *IL-8*, and *IL-18*), anti-inflammatory cytokines (*IL-10* and *TGFβ*), and a housekeeping gene (*TBP*) were not affected by exposure to MWCNTs (Figs. 4 and 5).

CB did not affect these cytokine mRNA expressions in peritoneal cells. For crocidolite-treated mice, sustained mRNA overexpression was observed only for an inflammatory cytokine gene, *IL-6* (4, 5, 6, and 8 times higher at the end of 2, 4, 10, and 20 weeks, respectively), which

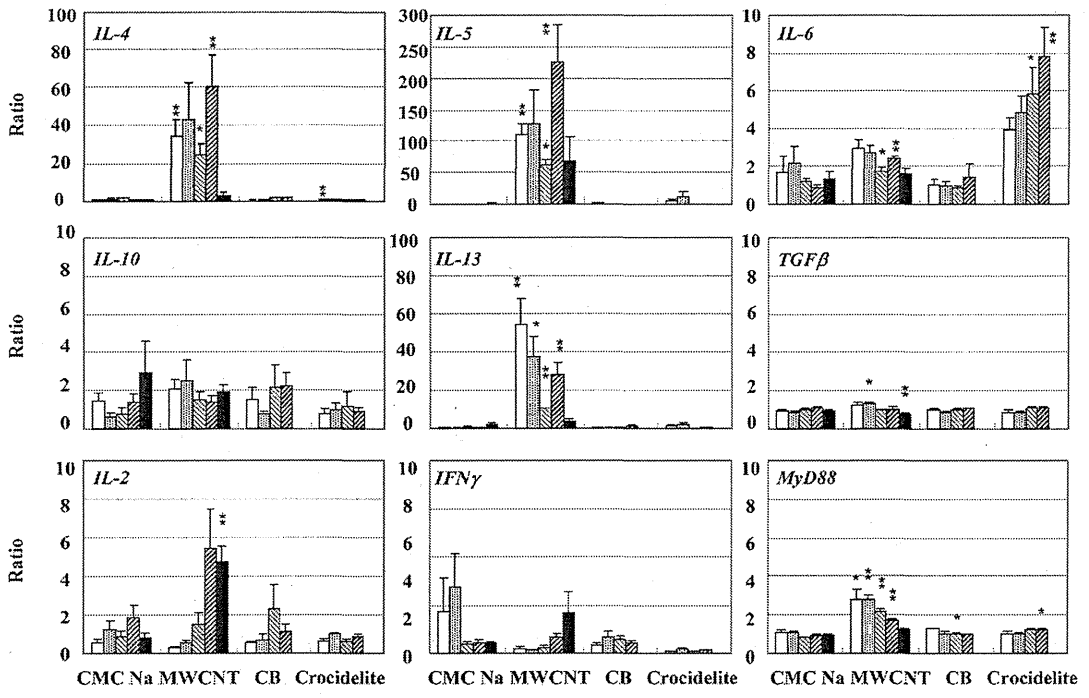

Fig. 4. mRNA expression of Th2 cytokine genes (*IL-4*, *IL-5*, *IL-10*, *IL-13*, and *TGFβ*), Th1 cytokine genes (*IL-2* and *IFNγ*), and a TLR adaptor protein (*MyD88*) in peritoneal cells obtained from mice in the first animal experiment. For each group of mice exposed to a test chemical or vehicle, columns from the left to the right are average values (n = 3-6) at 2, 4, 10, 20, and 34 weeks after exposure. These determinations were not made at the end of week 34 for the CB- and crocidolite-treated groups. (*$p < 0.05$, **$p < 0.01$).